High-Resolution Small Animal Imaging on 3T Clinical MR Scanners

Robin M. Heidemann[1], Deepu R. Pillai[2], Felix Schlachetzki[2], Thomas Steinberger[3], Titus Lanz[3], Ulrich Bogdahn[2]

[1] *Siemens Medical Solutions, Erlangen, Germany*
[2] *Dept. of Neurology, University Hospital of Regensburg, Regensburg, Germany*
[3] *RAPID Biomedical, Rimpar, Germany*

Introduction

Whenever the subject of small animal imaging comes up, people imply the use of dedicated small animal high field MR scanners with field strengths in the range of 7T to 17.6T. Currently, only few research facilities rely on conventional clinical MR scanners with field strengths of 1.5T to 3.0T for small animal studies. It is quite interesting to note that these “low field” systems also offer some advantages for small animal studies and a closer look at the options available can be of some importance.

In comparison to clinical MR scanners, dedicated small animal systems offer higher field strengths as well as stronger and faster gradients. This available high field strength directly translates into a higher signal-to-noise ratio (SNR) even though it comes at a price. There are four primary field-strength related effects which can diminish image quality.

Susceptibility effects: Living organisms are made up of various soft tissue types, air cavities and bones, all with different magnetic susceptibility values. Large susceptibility jumps, resulting from sudden transitions between tissues with significant susceptibility differences, can cause local field inhomogeneities in conjunc-tion with the high main field in MRI. These inhomogeneities, which scale with the magnetic field strength, act as addi-tional local gradients and are responsible for local deformations of the object ge-ometry in the resulting MRI image.

T2* relaxation: The MR signal in general decays with a time constant T2*, which is otherwise known as the apparent T2. In addition to the tissue-dependent transversal- or T2 relaxation of the underlying tissue, other effects are also included in this phenomenon. For instance, unavoidable inhomogeneities of the main magnetic field, the afore mentioned susceptibility jumps and effects such as flow and diffusion lead to a shortening in the relaxation time constant T2*. Whenever the readout train of an imaging sequence is not small compared to T2*, the T2* relaxation will affect the MR signal. Ultrafast imaging techniques like Echo Planar Imaging (EPI), Turbo Spin Echo (TSE) or HASTE are particularly plagued by a

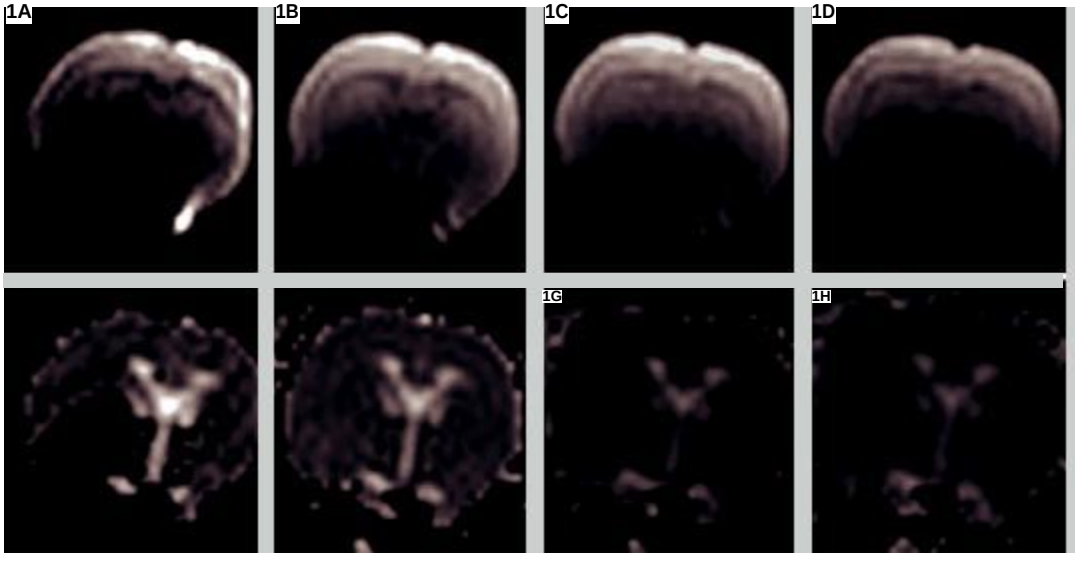

1 Single-shot diffusion-weighted (DW) EPI of the rat brain on a clinical MR scanner (MAGNETOM Allegra) at 3T using a 4-channel phased array head coil for the rat.

A–D: DW EPI with b = 1000 s/mm² using iPAT (*syngo* GRAPPA) with PAT factors of 1, 2, 3 and 4 (from A to D).

E–H: Corresponding ADC maps.

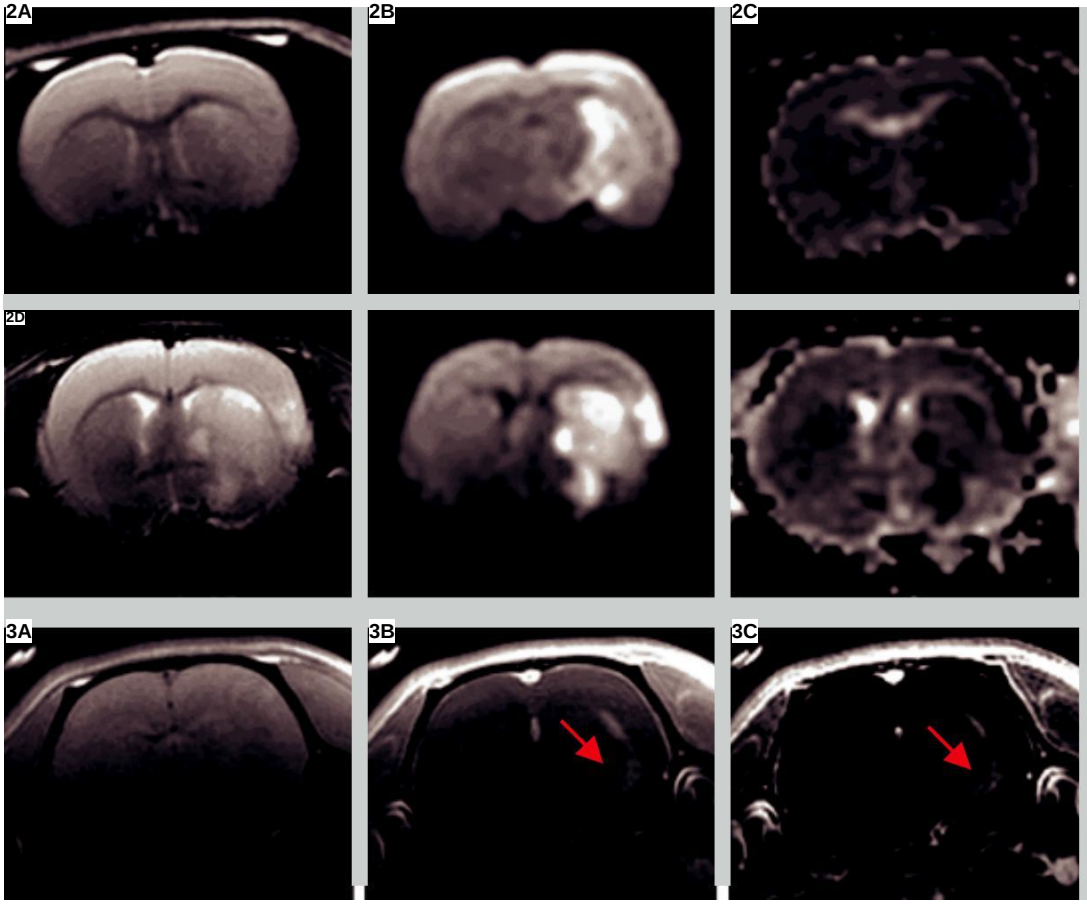

2 Small animal stroke imaging on a clinical MR scanner (MANGETOM Allegra) at 3T using a 4-channel phased array head coil for the rat.

A–C: Rat A, 6 h after occlu-sion.

D–F: Rat B, 36 h after occlusion. (A and D) *T2*-weighted TSE, (B and E) DW EPI with PAT factor 3, (C and F) corresponding ADC maps.

3 Small animal post-contrast study on a clinical MR scanner (MAGNETOM Allegra) at 3T using a 4-channel phased array head coil for the rat: Rat A, 8 h after occlusion. The arrow indicates MR contrast agent leakage.
A: Pre-contrast acquisition
B: Post-contrast acquisition 30 min after injection of the contrast agent.
C: Subtraction image demonstrates the region of the blood-brain-barrier (BBB) damage.

strong signal loss due to T2* relaxation. This signal attenuation is responsible for significant image blurring and produces a loss of small object contrast. The signal decay in high-field systems occurs much faster than at lower field strengths, as the T2* values at these higher fields are significantly shorter.

T1 relaxation: The magnetic field strength also affects the longitudinal or T1 relaxation. In general, there is no rule which describes the effect of the magnetic field on the T1 times of different tissues. These irregular and often unpredictable changes in T1 values lead to a different contrast behavior of MRI sequences at high field strength as compared to low field strength, which can be partially compensated by the use of a longer repetition time (TR), but this also implies a prolonged total acquisition time.

Specific absorption rate: Another high-field specific problem is the specific absorption rate (SAR), or the amount of energy (Watt x time) from high-frequency pulses absorbed by the body per unit time and weight. As an example, the transition from 1.5T to 3.0T generally increases the SAR value by a factor of four. In general, imaging protocols which run at low field strength have to be adapted for higher field strength to stay below the SAR limit, e.g. by the use of a longer TR, which also prolongs the total acquisition time.

It is clear that clinical low field systems cannot compete in terms of SNR with dedicated small animal high field systems, but the field strength related problems described above are smaller at lower field strengths. This is of major importance for examinations based on fast imaging tech-niques, such as EPI or HASTE. Further, the use of parallel imaging (integrated Paral-lel Acquisition Technique, iPAT), which is routinely available on clinical MR scanners, improves the image quality of such studies. The animal handling for the experimental set up is easier, because clinical scanners offer more space than dedicated small animal systems.

In this study, we demonstrate that high image quality small animal imaging on clinical MR scanners can be obtained in acquisition times comparable to those used for human examinations. This enables a direct transfer of findings and protocols from the small animal model onto human studies, performed on the same MR system. Short acquisition times directly translate into a higher throughput, which is of major importance for large small animal studies. Additionally, a short-er scan time means less stress for the animal itself, which will reduce the mortality rate. The properties of small animal imaging on clinical MR systems described above can finally be used to reduce the total costs of large small animal studies.

Methods

Animal care and all experimental procedures were conducted in accordance with German laws governing animal care and with the European Communities Council

Protocol	Standard human	Animal model
T2-weighted TSE	*0.6 x 0.4 x 5.0 mm* *1 min 20 s*	*0.2 x 0.2 x 1.5 mm* *2 min 18 s*
T1-weighted SE	*1.0 x 1.0 x 3.0 mm* *5 min 19 s*	*0.2 x 0.2 x 1.0 mm* *8 min 4 s*
DW EPI	*1.8 x 1.8 x 5.0 mm* *1 min 14 s*	*0.5 x 0.5 x 1.6 mm* *2 min 20 s*

Tab 1: Comparison between the standard MR protocols used for clinical human examinations and adapted small imaging protocols. The resolution and the total acquisition time are listed for the three protocols used for stroke examination.

Directive (86/609/EEC). Protocols were approved by the Ethics Committee for animal research of the local authorities.
All experiments were performed on 3T clinical MR scanners; either on a MAGNETOM Allegra (Siemens Medical Solutions, Erlangen, Germany) or on a MAGNETOM Trio, A Tim System (Siemens Medical Solutions, Erlangen, Germany). The Allegra was equipped with a 4-chan-nel phased array head coil and a 4-chan-nel phased array spine coil for the rat (RAPID Biomedical, Rimpar, Germany), while the Tim Trio was equipped with an 8-channel phased array whole body coil for the mouse (RAPID Biomedical, Rimpar, Germany).

Results

A conventional diffusion-weighted (DW) EPI examination of a healthy rat brain is shown in Fig. 1A. In comparison, Figs. 1B–1D show a series of DW EPI acquisitions with PAT factors from 2 to 4 using *syngo* GRAPPA [1]. The in-plane resolution being 500 µm and the slice thickness is 1.6 mm. Corresponding ADC maps can be found in the bottom row of Fig. 1.
Images obtained from a rat model of cerebral ischemia (Rat A, 6 h after Middle Cerebral Artery Occlusion (MCAO)) are shown in Figs. 2A–2C. While the images in Figs. 2D–2F are from a different rat (Rat B) acquired 36 hrs after occlusion. T2-weighted TSE images are shown in Fig. 2A and Fig. 2D. The in-plane resolution is 200 µm with a 1.5 mm slice thickness. The total acquisition time of the TSE study was 2 min 18 s, with 11 slices. The corresponding DW EPI (b = 1000 s/mm$_2$) images with a PAT factor of 3 are shown in Figs. 2B and 2E. The in-plane resolu-tion is 500 µm and the slice thickness is 1.6 mm. The total acquisition time of the DW EPI study with three directions and four b values was 2 min 20 s. Calculated ADC maps are shown in Figs. 2C and 2F.
Results from a post contrast T1-weighted study to detect the blood-brain-barrier (BBB) permeability can be seen in Fig. 3. The acquisition time of each examination was 8 min 4 s, with the same in plane resolution as for the TSE study. Table 1 shows a direct comparison between the standard and the adapted small animal protocol parameters, in terms of resolution and total acquisition time.
Images obtained from a small animal model of hemorrhagic stroke acquired 2 hrs after blood injection are shown in Fig. 4. A single slice from a T2-weighted TSE acquisition is shown in Fig. 4A. The in plane resolution is 200 µm with a 1.0 mm slice thickness. The total acquisition time of the TSE study with 11 slices using 3 averages was 2 min 18 s. The corresponding susceptibility-weighted image is shown in Fig. 4B. Here, the in plane resolution is 400 µm with 1.6 mm slice thickness. The total acquisition time of the T2*-weighted gradient echo (GRE) sequence with 11 slices, using 2 averages was 1 min 76 s.
Single sagittal sections from two animals of a spinal contusion injury are shown in Fig. 5. The T2-weighted TSE acquisitions have an in-plane resolution of 200 µm with a slice thickness of 400 µm. The total acquisition time of the TSE study using 3 averages and 11 slices in 2 concatenations was 5 min 35 s. These images were acquired without respiratory or cardiac gating, which would improve the overall image quality. A series of whole mouse images with PAT factors from 1 to 4 is shown in Fig. 6. Those images were obtained on a MAGNETOM Trio, A Tim System using an 8-channel phased array whole-body coil for the mouse. With the same set up, a contrast enhanced 3D FLASH acquisition was performed on a mouse with congested kidneys (Fig. 7). This study was obtained with a PAT factor of 2. The acquisition of this dataset with an isotropic resolution of 300 µm took about 4 min.

Discussion

In EPI the use of iPAT reduces blurring due to T2* relaxation and distortions due to off-resonance effects significantly [2]. It has been shown that this effect is especially important for stroke detection using DW EPI [3]. Further, the use of iPAT allows one to shorten the echo time (TE), in the example shown in Fig. 1, from 174 ms down to 77 ms. The reduction of TE increases the signal-to-noise ratio (SNR), which can balance out the inherent loss in SNR due to the use of iPAT in a certain range. The use of iPAT for DW EPI of small animals on a 3T clinical MR scanner is essential to obtain high image quality. In terms of off-resonance distortion reduction and achievable SNR, iPAT with an acceleration factor of 3 is found to perform best for this specific set up.
The feasibility of small animal imaging after experimental transient ischemia on a 3T clinical MR scanner is demonstrated in Figs. 2 and 3. High resolution, high quality images were obtained using standard Siemens product sequences with some protocol adaptations for the small

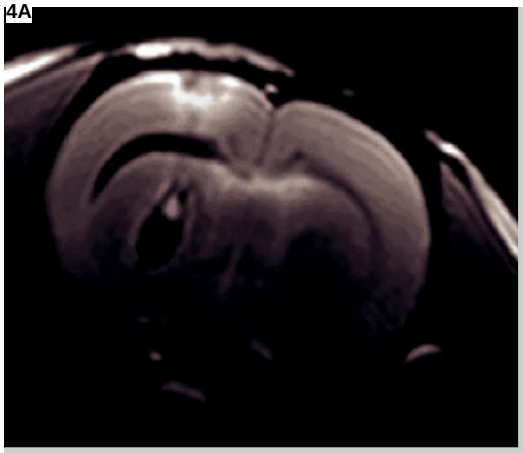

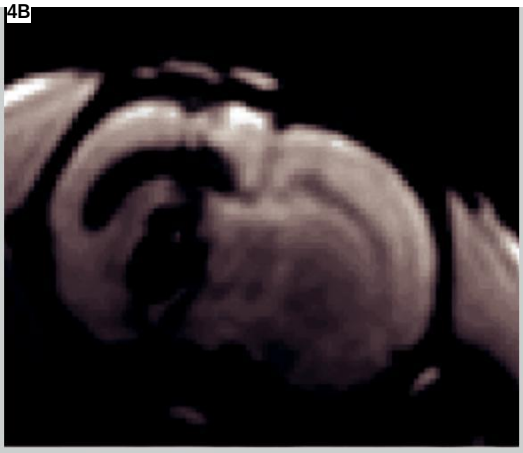

4 Small animal hemorrhagic stroke imaging on a clinical MR scanner (MAGNETOM Allegra) at 3T using a 4-channel phased array head coil for the rat:

A: T2-weighted TSE acquisition.

B: T2*-weighted GRE acquisi-tion.

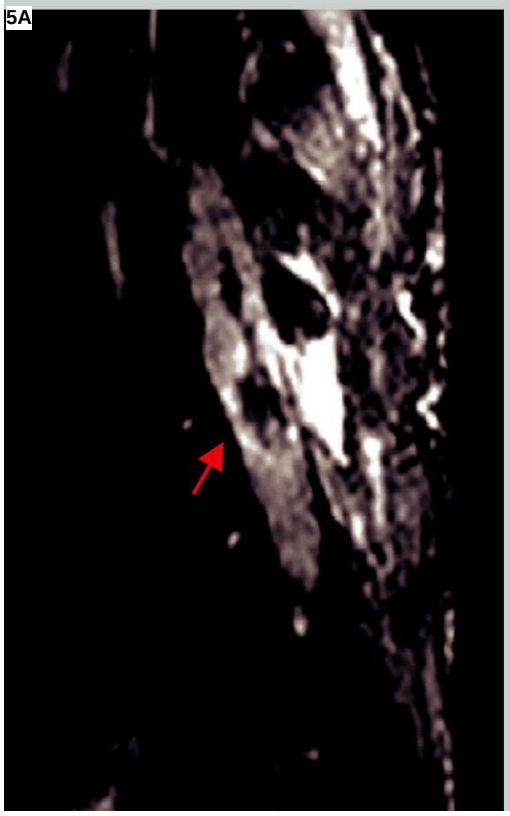

5 Imaging of spinal cord injury in rats on a clinical MR scanner (MAGNETOM Allegra) at 3T using a 4-channel phased array spine coil for the rat: T2-weighted TSE sequence with 200 µm in plane resolution and 400 µm slice thickness.

field of view and the high resolution. As shown in Table 1, the total acquisition time is comparable to standard imaging protocols used for human examinations. Besides a 4-channel phased array head coil for the rat and the animal handling system, no specific hardware had to be used. To achieve sufficient SNR in the high resolution small animal experiments, it was necessary to use more averages or to turn off the partial Fourier option, which explains the longer acquisition times compared to the standard human protocols. As can be seen in Fig. 6, the use of iPAT in combination with the HASTE sequence [4] helps to increase the resolution of those acquisitions.

Conclusion

High resolution small animal imaging on 3T clinical MR scanners can be realized in scan times comparable to those used for human examinations. Since all imaging protocol parameters fall in a tolerable range for human applications, a direct transfer of the knowledge gained with those small animal models to human studies is possible.
The short acquisition times can be used to increase the animal throughput of the system and can reduce the mortality rate due to examination stress. Finally, this approach can reduce the overall cost of studies with a large number of small animals being examined.

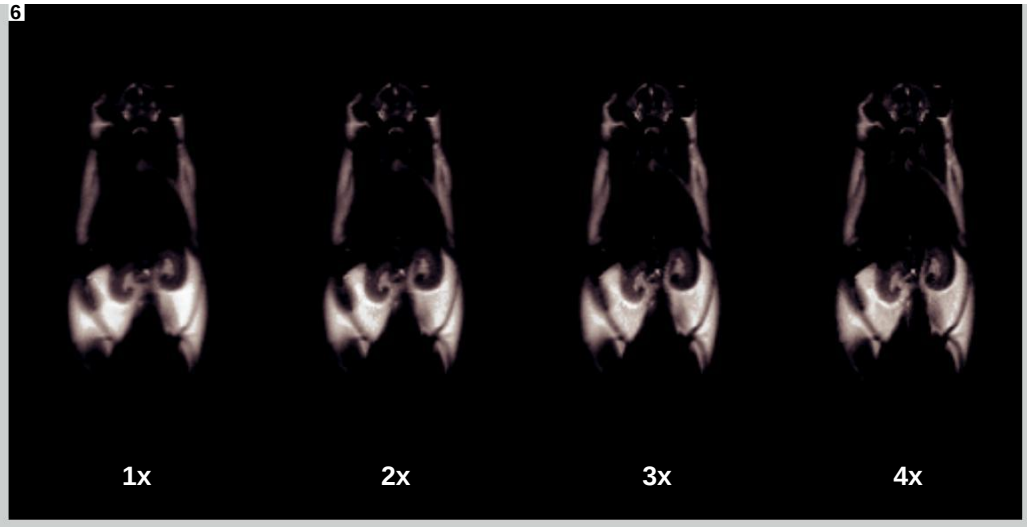

6 Imaging of a whole mouse on a clinical MR scanner (MAGNETOM Trio, A Tim System) at 3T using an 8-channel phased array Body Matrix coil for the mouse: T2-weighted HASTE sequence with PAT accelera-tion factors from 1 to 4.

Images courtesy of Herbert Reinl, Grosshadern, Munic, Germany.

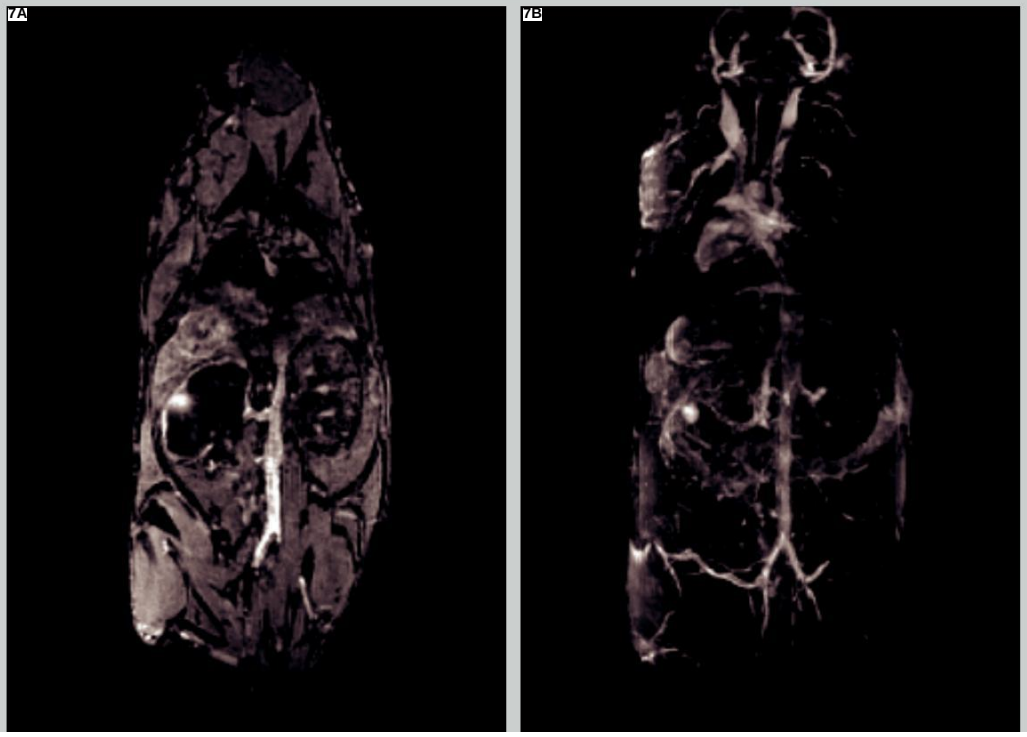

7 Imaging of a whole mouse with congested kidneys on a clinical MR scanner (MAGNETOM Trio, A Tim System) at 3T using an 8-channel phased array whole-body coil for the mouse: 3D FLASH with PAT factor 2.

Images courtesy of Herbert Reinl, Grosshadern, Munic, Germany.

Acknowledgement

This work was supported by Siemens Medical Solutions and the Bavarian Re-search Foundation (Grant 570/3).

References

1 Griswold MA, Jakob PM, Heidemann RM, Nittka M, Jellus V, Wang J, Kiefer B, Haase A. Generalized autocalibrating partially parallel acquisitions (GRAPPA). Magn Reson Med 2002; 47: 1202–1210.

2 Griswold MA, Jakob PM, Chen Q, Goldfarb J, Manning WJ, Edelman RR, Sodickson DK. Resolution enhancement in single-shot imaging using simulta-neous acquisition of spatial harmonics (SMASH). Magn Reson Med 1999; 41: 1236 –1245.

3 Bammer R, Keeling SL, Augustin M, Pruessmann KP, Wolf R, Stollberger R, Hartung HP, Fazekas F. Improved diffusion-weighted single-shot echo-planar imaging (EPI) in stroke using sensitivity encoding (SENSE). Magn Reson Med 2001; 46: 548–554.

4 Heidemann RM, Griswold MA, Kiefer B, Nittka M, Wang J, Jellus V, Jakob PM. Resolution enhancement in lung ^{1}H imaging using parallel imaging methods. Magn Reson Med 2003; 49: 391–394.